

Water Transport in Graphite/Epoxy Composites

MYUNG CHEON LEE* and NIKOLAOS A. PEPPAS†

School of Chemical Engineering, Purdue University, West Lafayette, Indiana 47907

SYNOPSIS

The diffusive and mechanical behavior of tetraglycidyl diaminodiphenyl methane (TGDDM) resin-based composites and diglycidyl ether of bisphenol-A (DGEBA) resin-based graphite/epoxy composites were investigated during water sorption at different temperatures. The water-absorption kinetics in both systems at 50, 70, 90, and 100°C were fitted by a Fickian diffusion model. However, a Langmuir-type, two-step sorption behavior was observed for water transport in DGEBA-based systems at 50 and 70°C. Using scanning electron microscopy, internal cracks due to water absorption were found in the DGEBA-based samples after conditioning at 90 and 100°C in water, whereas no cracks were detected in TGDDM-based samples conditioned in water at 100°C. Ultrasonic testing did not show significant modulus or density change of the TGDDM-based samples conditioned in water at 100°C. No significant changes of dynamic modulus or damping factor were observed for the TGDDM-based samples redried after immersion in 100°C water, whereas slight changes were observed above 120°C for the samples containing absorbed water. However, both water-containing and redried DGEBA-based samples showed a decrease of dynamic modulus and an ω -transition around 120°C. A single-fiber fragment test revealed that the absorbed water at 80°C reduced significantly the interfacial shear strength of DGEBA/DDA resin-AS4 fiber samples and DGEBA/DDA resin-AU4 fiber samples. © 1993 John Wiley & Sons, Inc.

INTRODUCTION

Composites based on epoxy resins are widely used in a variety of applications, especially in the aerospace industry. Prepreg matrices based on tetraglycidyl-4,4'-diaminodiphenyl methane (TGDDM) epoxy resins with graphite fibers can be cured to form composites with superior mechanical properties.¹ Diglycidyl ether of bisphenol A (DGEBA) and epoxy Novolac compounds are also widely used. Uncured epoxide resins are usually cured with cross-linking agents that have at least two reactive amine groups. The mechanical properties of the cured epoxy resins can be altered depending on the cross-linking agent used, the selection of the proper curing time and temperature, as well as processing methods

for minimization of the presence of voids in the composites.

The epoxy resins used in such systems usually absorb water or moisture. This moisture absorption can be attributed largely to the water affinity for specific functional groups of the cured epoxy resin of a highly polar nature. The most widely cited evidence for this affinity is measurement of water in epoxy resins² and epoxy composites³ using NMR spectroscopy. Since the NMR line width decreases with increasing molecular mobility, the broadening spectrum of water in epoxy resins indicates that water is hydrogen-bonded to the resin; its mobility in epoxy resins is between the solid- and free-water states. Using FTIR spectroscopy, Antoon et al.⁴ showed that the frequency of the in-plane bending mode of water in epoxy resins lies between the frequencies of liquid and free water. Therefore, they proposed that the sorbed water was held within the epoxy resin by hydrogen bonding.

Karasz and co-workers^{5,6} investigated the nature of the epoxy-water molecule interactions using

* Present address: Department of Chemical Engineering, Dukgong University, Seoul, Republic of Korea.

† To whom correspondence should be addressed.

quadrupole echo deuterium NMR spectroscopy. They revealed that (i) the water in epoxy resin is impeded in its movement; (ii) there is no free water; (iii) there is no evidence for tightly bound water; and (iv) it is unlikely that water disrupts the hydrogen-bonded network in the epoxy resin. Using dielectric experiments, Woo and Piggott⁷ suggested that the water does not appear to be bound to polar groups in the resin or hydrogen-bonding sites. They reported that there was only some clustering of water molecules in the polymer, rather than complete separation of molecules.

Apicella et al.^{8,9} proposed that there are three modes of sorption: (i) bulk dissolution of water in the polymer network; (ii) moisture absorption onto the surface of holes that define the excess free volume of the glassy structure; and (iii) hydrogen bonding between hydrophilic groups of the polymer and water. If the first two modes occur consecutively, a dual sorption behavior can be observed.

Moisture absorption or cyclic absorption and desorption at high temperatures and relative humidities can cause voids and/or microcracks in the epoxy resin. If these effects are extensive, conditions for non-Fickian transport can be induced. Thus, we can expect either non-Fickian or Fickian transport depending on the resin properties and environmental conditions. Various studies have revealed that the moisture transport in composites can be described by a Fickian diffusion model with a constant,¹⁰ a concentration-dependent,¹¹ or a stress-dependent diffusion coefficient.¹¹

When an epoxy resin absorbs water, the local degree of water sorption (swelling) depends on the local water concentration. As a result, the more "swollen" regions experience a compressive force, whereas less "swollen" regions experience tensile forces. The tensile stress can enhance the water transport rate. Such a self-induced stress can cause a non-Fickian behavior. Farrar and Ashbee¹² found that the water-transport rate under this self-induced stress is an order of magnitude greater than the rate without stress.

Several researchers^{13,14} observed that the hygrothermal conditions can cause an interfacial debonding in glass fiber/epoxy resin composites. In graphite/epoxy composites, Kaelble et al.^{15,16} observed that the interlaminar shear strength could be reduced by 30–50% after immersion for 200 h in 100°C water. They suggested that this degradation is irreversible and is directly related to cumulative moisture degradation of the fiber–matrix interfacial bond. Tsotsis and Weitsman¹⁷ calculated the energy-release rate in microcrack formation due to moisture

absorption in graphite/epoxy composites. They suggested that moisture weakened the fiber/matrix interface by reducing the adhesion and creating damage around the fiber.

In the present work, experiments were performed on two types of epoxy composites to investigate the influence of water transport in the debonding between matrix and fiber, to analyze the mechanism of water transport, and to associate the developing stresses at the matrix/fiber interface to the debonding between the two components.

EXPERIMENTAL

Materials Preparation

The epoxy composites used in this work were Hercules AS4/3501-6 and Fiberite ANC3K/948A1. The Hercules 3501-6 epoxy resin contains 88.5 wt % tetraglycidyl diamine diphenol methane (TGDDM) and 11.5 wt % Novolac with 25 phr (part per hundred parts of epoxy) diamino diphenyl sulfone (DDS) and 2 phr boron trifluoride complexed with monoethylamine (BF₃MEA). The Fiberite 948A1 epoxy resin consists of diglycidyl ether of bisphenol-A (DGEBA) epoxy, dicyandiamide (DDA) cross-linking agent, and 4-chlorophenyl urea catalyst.

Both composite samples were prepared by curing prepregs laid up on a mold in the same direction to make a unidirectional laminate. An autoclave vacuum-bag curing method was used for their preparation. Curing of the TGDDM-based composite sample was done by sealing the prepreg inside a vacuum bag with the vacuum set at 0.16 atm. The temperature of the autoclave was raised to 116°C at 2°C/min and the autoclave was pressurized to 586 kPa at 116°C. This temperature was then held for 70 min at 586 kPa while the vacuum of the vacuum bag was maintained. The temperature was then raised to 177°C at 2°C/min and maintained at 177°C for 2.2 h. After the isothermal curing, the sample was cooled to 66°C in 2 h and was finally postcured at 177°C for 3.5 h. These conditions are similar to industrial conditions for the preparation of such systems.

Curing of the DGEBA-based composite sample was carried out the same way as before while the temperature of the autoclave was raised to 127°C from the room temperature for 1 h. This temperature was held for 2 h and then cooled down to room temperature for 1 h; this sample was not postcured, as typically done in industry.

Water-Sorption Tests

Samples with identical properties and curing history were cut from the same composite panel. The sample size was $4 \times 4 \text{ cm}^2$, and the thickness was 0.075 cm for Hercules composite samples and 0.04 cm for Fiberite ones. The ratio of sample side area to the main surface area was 3.75% for Hercules composite samples and 2.0% for Fiberite composite samples. Therefore, side sorption effects were assumed to be negligible.

After measuring the initial weight of each sample, the slabs were submerged in deionized water in 100 mL vials. Gravimetric studies were performed at 50, 70, and 100°C. The experimental error of this test is usually $\pm 0.01\%$.

Hygrothermal Effects

The physical effects of hygrothermal conditions were studied using photomicrography, scanning electron microscopy, ultrasonic testing, and dynamic viscoelasticity. A single-fiber fragment test and infrared spectroscopy were applied to investigate the hygrothermal effects on the fiber/resin interfacial bonding.

To investigate the hygrothermally induced damages in both Hercules AS4/3501-6 and Fiberite ANC3K/948A1 composites, the samples were immersed in 50, 70, 90, and 100°C water for up to 1200 h. Micrographs were taken with a 35 mm camera having a contact lens. After immersion in water, the samples were removed and cut transversely to the fiber direction. The cross-sectional area was investigated with a scanning electron microscope.

In the ultrasonic testing procedure, the change of ultrasonic wave velocity was measured at the frequency of 150 kHz and at room temperature. Two types of unidirectional Hercules AS4/3501-6 composite samples were prepared. In one sample, the wave propagated in the same direction with the fiber to measure the longitudinal wave velocity. In the other sample, the wave propagated transversely to the fiber to measure the transverse wave velocity. The length of the samples was 10 cm and the thickness was 0.75 mm. To investigate hygrothermal effects, the samples were immersed in 100°C water and were taken out periodically to measure the wave velocities.

Dynamic mechanical tests were performed using a dynamic viscoelastometer (Rheovibron, Toyo Baldwin, model DDVII-C, Tokyo, Japan). Dynamic modulus and $\tan \delta$ were measured as a function of temperature at 3.5 Hz. Samples were unidirectional

fiber composites and the dynamic forces were applied transversely to the fiber direction. Two types of experiments were performed. Samples containing various amounts of water were prepared to investigate the influence of water on the dynamic mechanical properties, whereas redried samples after various periods of hot-water conditioning were prepared to investigate hygrothermally induced degradation. For the first test, dry samples as well as samples of Hercules AS4/3501-6 containing 0.60, 1.07, and 1.57 wt % water were used along with Fiberite ANC3K/948A1 samples containing 0.87, 1.36, and 1.87 wt % water. To prevent water desorption from the samples during dynamic tests, they were coated by silicon vacuum grease. There was no absorption of water by the vacuum grease. To test water degradation, samples were immersed in 100°C (Hercules AS4/3501-6) and 90°C (Fiberite ANC3K/948A1) water for 4, 11, and 21 days and then redried in vacuum oven for 5 days at 85°C.

To further investigate the influence of water, surface-treated Hercules AS4 fibers and nontreated Hercules AU4 fibers were prepared. TGDDM epoxy resin, MY 720, was mixed with 25 phr DDS hardener and a DGEBA epoxy resin, Epon 828, was mixed with 12 phr DDA hardener.

For the fiber fragment test, standard epoxy tensile samples were prepared using a silicon rubber mold. First, both ends of fiber were fixed to both ends of the mold with an instant epoxy adhesive. The epoxy resin mixed with a curing agent was then carefully cast into the mold. Curing was done in an oven at 121°C for 70 min and then at 177°C for 150 min in the case of TGDDM and DDS system and at 127°C for 80 min in case of the DGEBA and DDA system.

The TGDDM/DDS samples were immersed in 100°C water, whereas the DGEBA/DDA samples were immersed in 70°C water for 4, 7, or 11 days. Constant strain rate, $1.814 \times 10^{-5} \text{ cm/s}$, was applied to the sample by an MTS machine until there was no change of the length of fiber fragments. The length of fiber fragments within gauge length was measured by microscopy.

RESULTS AND DISCUSSION

Water-Sorption Kinetics

To study the water-sorption kinetics, water-uptake curves were obtained for various conditions. Figure 1 shows the normalized sorption data for TGDDM/DDS-based composites (Hercules AS4/3501-6) at 50, 70, 90, and 100°C. As the temperature increased

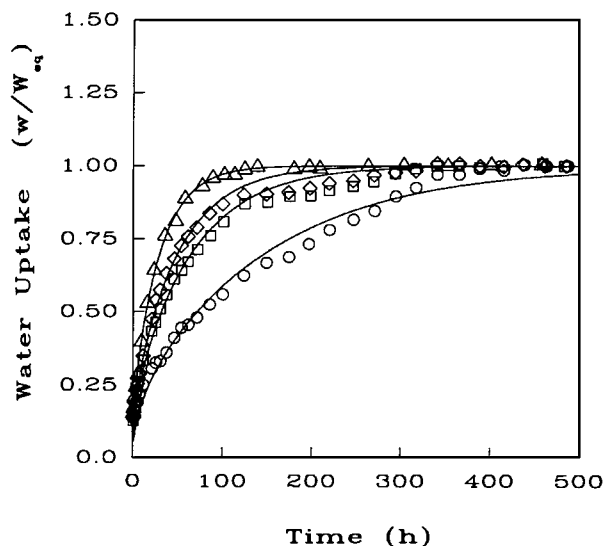


Figure 1 Normalized water uptake as a function of time for four different temperatures in Hercules AS4/3501-6 samples: (○) 50°C; (□) 70°C; (◇) 90°C; (△) 100°C. Curves indicate the prediction of Fickian model [eq. (1)].

from 70 to 100°C, the sorption rate increased, while relatively more increase was observed from 50 to 70°C. Data were fitted with a Fickian sorption model¹⁸ as expressed by the simple solution of eq. (1) under constant diffusion coefficient and with initial water concentration of zero through the composite and constant (zero) at the composite/water interface:

$$\frac{\partial c}{\partial x} = D \frac{\partial^2 c}{\partial x^2} \quad (1)$$

The curves of Figure 1 represent the fitting results at each temperature. It appears that the water sorption behavior in the Hercules AS4/3501-6 composite can be predicted well by a Fickian sorption model. The diffusivities at each temperature were of the order of 10^{-9} cm²/s and are listed in Table I. Figure 2 shows the normalized sorption data of DGEBA/DDA-based (Fiberite ANC3K/948A1) composites at 50, 70, 90, and 100°C. As the temperature increased from 70 to 100°C, the sorption rate increased.

A Langmuir-type two-step model [eqs. (2) and (3)] could best fit the sorption data at 50 and 70°C, while a Fickian model could best fit the data at 90 and 100°C. The Langmuir-type two-step model can be represented by eqs. (2) and (3):

$$D \frac{\partial^2 n}{\partial x^2} = \frac{\partial n}{\partial t} + \frac{\partial N}{\partial t} \quad (2)$$

$$\frac{\partial N}{\partial t} = \gamma n - \beta N \quad (3)$$

Here, D is the diffusion coefficient of mobile molecules; n , the number density of mobile molecules; N , the number density of bound molecules; and γ and β , constants expressing the probability that water is bound per unit time.¹⁸

The order of magnitude of Fickian diffusion coefficient was 10^{-6} cm²/s at 90 and 100°C. Both Fickian diffusion coefficients are listed in Table I. The results of the data fitting at 50 and 70°C with a Langmuir type two-step model¹⁸ are presented in Table II.

Table I Water Absorption in Various Composites and Equilibrium Water Uptake at Various Temperatures

Composite Material	Temperature (°C)	Water Diffusion Coefficient (cm ² /s)	Equilibrium Water Uptake (g water/g resin)
TGDDM/DDS-based composite (Hercules)	50	0.9×10^{-9}	0.8
	70	2.1×10^{-9}	1.1
	90	2.8×10^{-9}	1.3
	100	4.7×10^{-9}	1.3
DGEBA/DDA-based composite (Fiberite)	50	nc	1.5
	70	nc	2.4
	90	8.2×10^{-6}	2.9
	100	10.4×10^{-6}	2.9

nc: Not calculated due to insufficient data points.

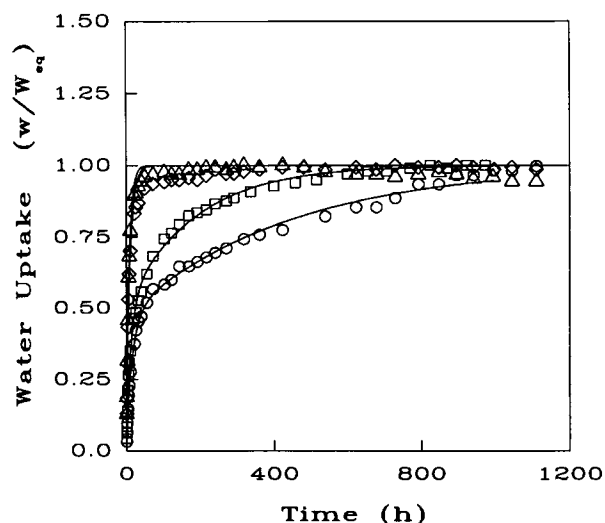


Figure 2 Normalized water uptake as a function of time for four different temperatures in Fiberite ANC3K/948A1 samples: (○) 50°C; (□) 70°C; (◇) 90°C; (△) 100°C. Curves for circles and squares indicate the prediction of Fickian model [eq. (1)], whereas those for diamonds and triangles indicate the prediction of the Langmuir-type two-step model [eqs. (2) and (3)].

Hygrothermal Effects

Water transport in the TGDDM/DDS-based Hercules AS4/3501-6 composite caused no surface damage at any of the experimental temperatures. No clear cracks were observed at the cross-sectional area of the samples using scanning electron microscopy. However, in the case of DGEBA/DDA-based Fiberite ANC3K/948A1 composite samples, some blisters of the sample surface were observed after 7 days immersion in 90 and 100°C.

Figure 3 shows the surface change of the Fiberite ANC3K/948A1 composite after 15 days in 90°C water. A number of blisters was seen at the surface of the sample. Each sample was then cut and the cross-sectional shapes of the blisters near the surface or the center region of the sample were observed (Fig. 4). This figure reveals that the blisters are caused by cracks. It is noticeable that the crack near the center is much larger than that near the surface region. According to the numerical simulation results of water-induced transient stress distribution,¹⁸ the tensile stress is always maximum at the center of the sample. Therefore, the simulation results support the explanation that a crack near the center region is larger than one near the surface region.

Changes of longitudinal ultrasonic wave velocity, v_l , and the transverse ultrasonic wave velocity, v_t , are shown for water transport in Hercules AS4/

3501-6 samples as a function of conditioning time (see Fig. 5). The trends of wave velocity as a function of conditioning time were not significant. Other researchers^{19,20} have noted a similar lack of trend of wave velocity in TGDDM-based graphite fiber composites upon water sorption at 100°C. These results suggest that the TGDDM-based graphite fiber composites are not affected significantly by immersion in 100°C water over 150 days. The longitudinal wave velocity was approximately 3.5 times faster than was the transverse wave velocity. Therefore, if no change of density is assumed, the longitudinal modulus of unidirectional Hercules AS4/3501-6 is 12.3 times higher than the transverse modulus.

The changes of dynamic modulus and $\tan \delta$ of Hercules AS4/3501-6 sample with varying water content as a function of temperature are shown in Figure 6. Both graphs show that the absorbed water caused a plasticizing effect by decreasing the modulus and increasing the $\tan \delta$ value. In $\tan \delta$ vs. temperature graphs, the plasticizing effect was clear around 120 to 200°C.

Several investigators have considered the temperature defined by the damping peak as the glass transition temperature. However, it is known that the glass transition temperature measured by dilatometry or DSC is 5–25°C lower than the temperature of the damping peak. The damping peak always coincides with the point of inflection of the modulus vs. the temperature curve. Therefore, it is reasonable to consider the intersection of two tangential lines of the modulus vs. the temperature curve as the glass transition temperature. As a result of this analysis, the glass transition temperature was calculated as 210°C, which is 20°C lower than the damping peak temperature.

In Figure 7, the changes of dynamic modulus and $\tan \delta$ of Fiberite ANC3K/948A1 containing various amount of water are represented as a function of temperature. In both graphs, the plasticizing effect for a Fiberite composite sample was more significant than for the Hercules composite sample. An interesting point in this Fiberite composite system is that minor inflection points in the dynamic modulus vs.

Table II Langmuir-Type Two-Step Model for Water Absorption by the Fiberite Composite

Temperature (°C)	D (cm ² /s)	β	γ
50	2.4×10^{-9}	2.5×10^{-3}	2.3×10^{-3}
70	3.0×10^{-9}	5.0×10^{-3}	5.4×10^{-3}

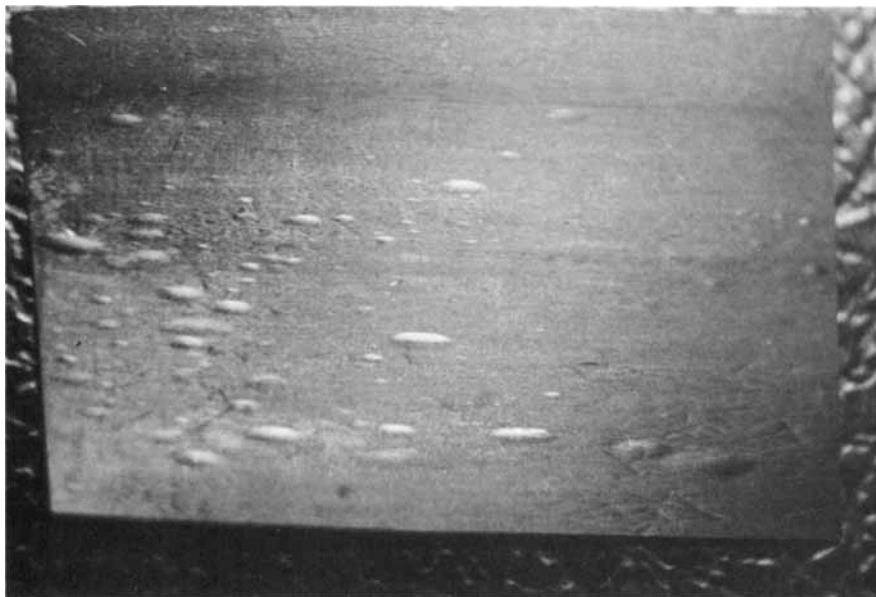


Figure 3 Surface change of Fiberite ANC-3K/948A1 after 15 days at 90°C water.

the temperature graph around 110°C and the minor transition points in $\tan \delta$ vs. the temperature graph around 110°C are observed for 1.36 and 1.87 wt % water-containing samples. This minor transition implies that the absorbed water has some effect on the rearrangement of the epoxy resin molecules. The dynamic modulus vs. the temperature curve indicates that the major glass transition temperature around 150°C is affected only minimally by absorbed water. Minor transition temperatures were observed around 90°C for samples containing 1.36 and 1.87 wt % water. The minor transition temperature of 110°C in the $\tan \delta$ vs. the temperature curve coincides with the temperature that Mikols et al.²¹ already reported for the water-soaked DGEBA-TETA epoxy resin system. Major damping peak temperatures were found around 165°C and a slight decrease (4–5°C) of major damping peak temperature was observed for samples containing 1.87 wt % water. In Figure 6, the plasticizing effect of water was evident even above 200°C.

To investigate if hygrothermal conditions can cause irreversible degradation on these composite materials, redried samples were tested after various periods of hygrothermal conditioning to determine the dynamic modulus and $\tan \delta$ as functions of temperature. Figure 8 shows the dynamic modulus and $\tan \delta$ of redried Hercules AS4/3501-6 samples after various periods of immersion in 100°C water as functions of temperature. In the dynamic modulus vs. the temperature curve, no degradation was ob-

served. However, a small plasticizing effect and a small increasing trend of the maximum $\tan \delta$ peak with increased conditioning period were observed around 180°C. The increasing trend of the maximum $\tan \delta$ peak can be caused by structural degradations such as crazes or microcavities in the epoxy resin and/or by degradation of the interfacial bonding between the epoxy resin and the graphite fiber. Several investigators^{22,23} have shown that the weakening of the interfacial bonding in various composite systems is associated with a trend of $\tan \delta$ to increase with temperature. The Fiberite ANC3K/948A1 samples showed a higher plasticizing effect above 100°C and a slightly higher trend of the maximum $\tan \delta$ peak as shown in Figure 9. The degradation of the epoxy resin and/or the interfacial bonding as well as the plasticizing effect could contribute the an increase of $\tan \delta$ above 100°C.

The change of the $\tan \delta$ peaks of both Hercules and Fiberite samples with various conditioning periods are plotted in Figure 10. In this figure, a 10% increase of the maximum $\tan \delta$ for the Hercules AS4/3501-6 sample and a 15% increase for the Fiberite ANC3K/948A1 sample are observed after 21 days of hygrothermal conditioning.

Single-Fiber Fragment Tests

The single-fiber fragment test may give information about the interfacial bonding at the matrix/fiber

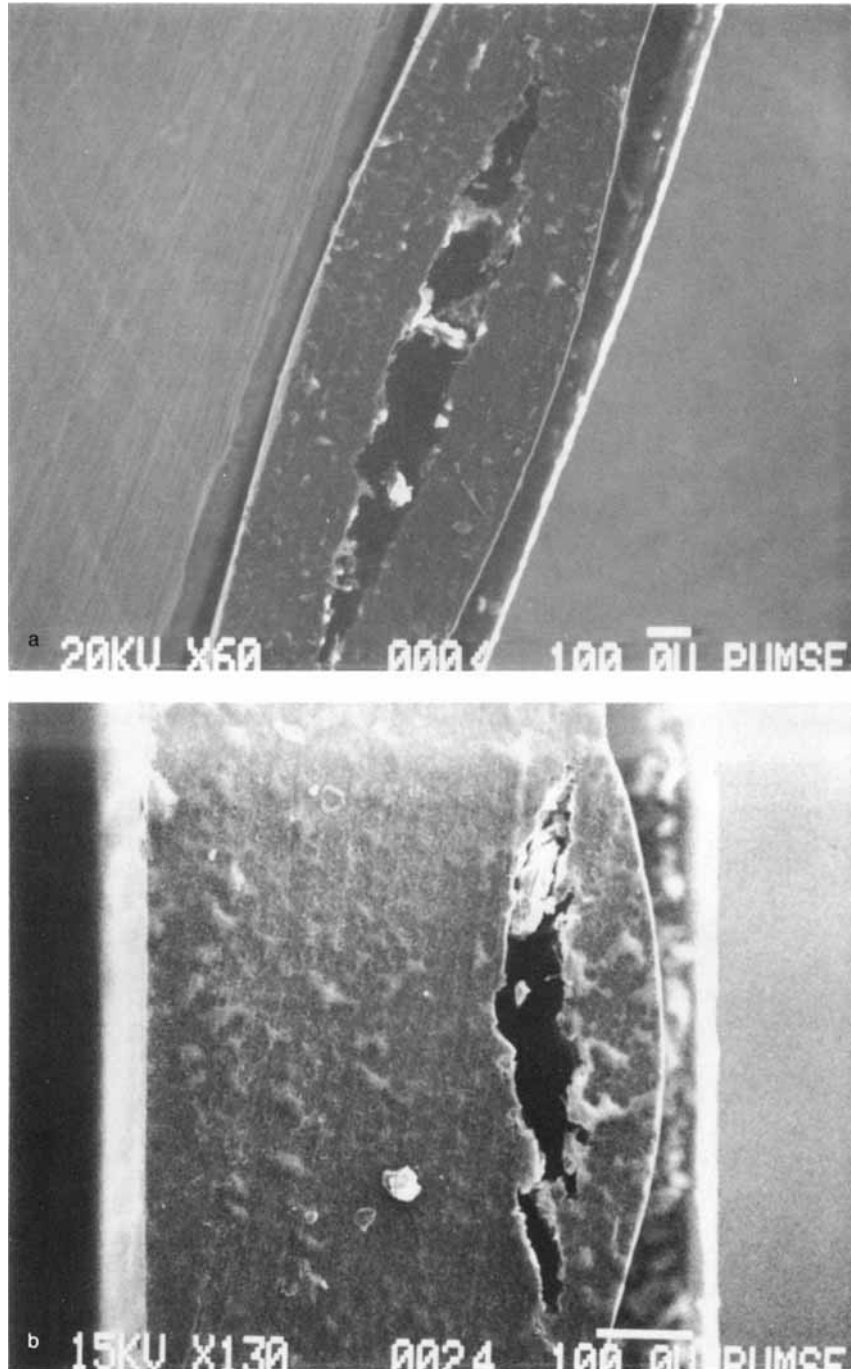


Figure 4 Crack in Fiberite ANC-3K/948A1 after 15 days at 90°C water: (a) crack at the center; (b) crack near the surface.

interface. For a single fiber embedded in a matrix, if the matrix is a perfect plastic material and the fiber is stretched by the shear forces acting at the interface,²⁴ the force balance at the interface²⁵ gives

$$\sigma_f \pi r^2 = 2\pi r l \tau_y \quad (4)$$

Here, σ_f is the fiber tensile stress, τ_y , the shear stress at the interface; r , the radius of fiber; and l , the distance from the fiber end. If the tensile stress builds up to the ultimate fiber tensile strength, σ_{fm} , the fiber breaks and a critical fiber length l_c will be reached. At equilibrium, eq. (4) can be altered to give the following equation:

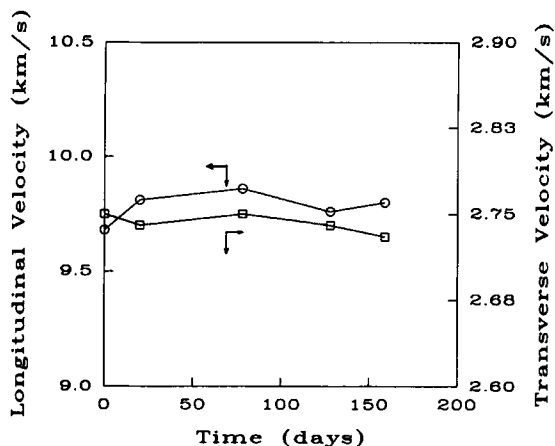


Figure 5 The change of ultrasonic wave velocities in Hercules AS4/3501-6 sample as a function of conditioning time.

$$\tau_y = \frac{\sigma_{fm} r}{2 l_c} \quad (5)$$

The distribution of critical fiber lengths can be best analyzed by a two-parameter Weibull distribution function, where α_2 and β_w are Weibull parameters:

$$F(x) = 1 - \exp\left[-\left(\frac{x}{\beta_w}\right)^{\alpha_w}\right] \quad (6)$$

Using eqs. (5) and (6), the most probable value of the interfacial shear strength can be written by eq. (7), where Γ is a gamma function:

$$\tau_y = \frac{\sigma_{fu}}{2\beta} \Gamma\left(1 - \frac{1}{\alpha}\right) \quad (7)$$

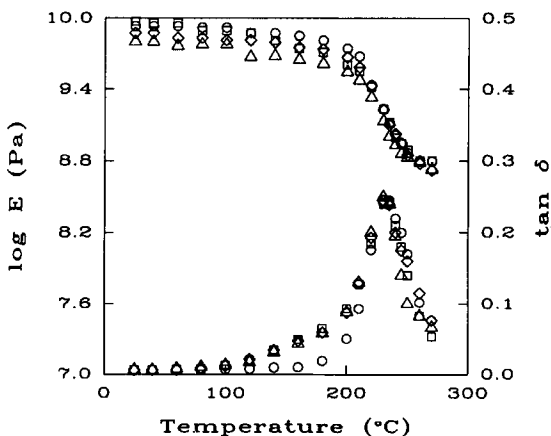


Figure 6 Dynamic modulus and $\tan \delta$ of Hercules AS4/3501-6 sample with various water contents as a function of temperature: (○) dry sample; (□) 0.6 wt % water; (◇) 1.0 wt % water; (△) 1.5 wt % water.

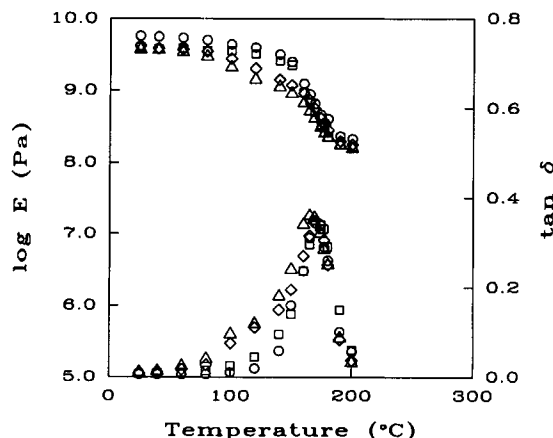


Figure 7 Dynamic modulus and $\tan \delta$ of Fiberite ANC3K/948A1 sample with various water contents as a function of temperature: (○) dry sample; (□) 0.87 wt % water; (◇) 1.36 wt % water; (△) 1.87 wt % water.

At room temperature, both TGDDM/DDS and DGEBA/DDA epoxy samples are too brittle to create enough strain for fiber breakage; the maximum strain was around 1.0%. As a result, all samples broke before the fibers broke. To attain high strain, tests were done at elevated temperatures. TGDDM/DDS samples could not attain sufficient strains for fiber breakage even at 200°C. DGEBA/DDA samples exhibited 4–5% strain at 80°C. Each tensile test was repeated three times at the same condition.

The tensile strength values of AS4 fiber (2.96 MPa) and AU4 (2.61 MPa) were used to calculate the interfacial shear strength. The diameters of AS4 and AU4 fibers were 0.7 μm as measured by mi-

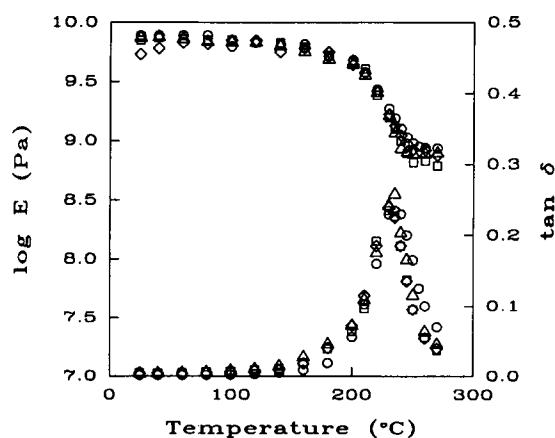


Figure 8 Dynamic modulus and $\tan \delta$ of redried Hercules AS4/3501-6 sample after various immersion time in 100°C water as a function of temperature: (○) non-conditioned; (□) 4 days; (◇) 11 days; (△) 21 days.

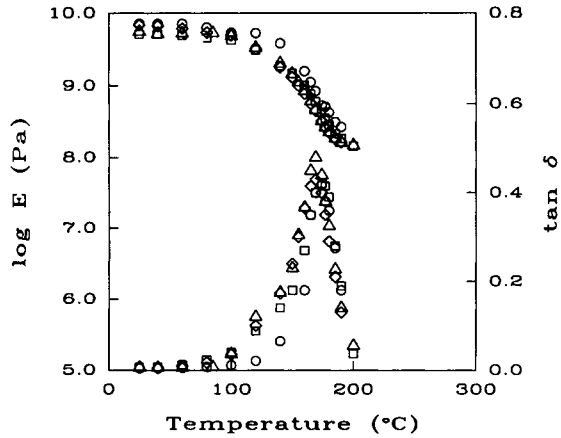


Figure 9 Dynamic modulus and $\tan \delta$ of redried Fiberite ANC3K/948A1 sample after various immersion time in 90°C water as a function of temperature: (○) nonconditioned; (□) 4 days; (◇) 11 days; (△) 21 days.

croscopy. The calculation results are summarized in Table III. In addition, the change of interfacial shear strength as a function of conditioning time is shown in Figure 11.

It is shown in Figure 11 that, before water conditioning, the interfacial shear strength of an AS4-DGEBA sample was 1.5 times higher than that of an AU4-DGEBA sample. The higher value of the interfacial shear strength of AS4-DGEBA samples can be explained by the surface-treating process. The surface-treating effects can include removal of fiber-surface defects, increase of effective surface area of the fiber, and providing of electrostatic and chemical

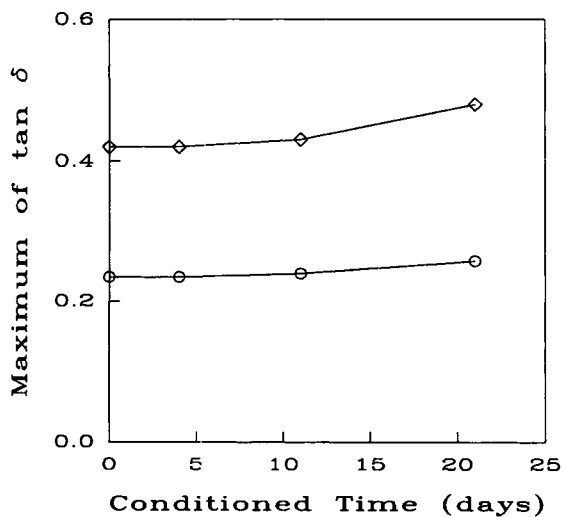


Figure 10 Maximum of $\tan \delta$ as a function of immersion time in 90°C water (Fiberite ANC3K/948A1) and 100°C water (Hercules AS4/3501-6).

Table III Interfacial Shear Strengths and Weibull Constants for Single-Fiber Fragment Test

Immersion Time (days)	AS4-DGEBA Composite (MPa)			AU4-DGEBA Composite (MPa)		
	α	β	τ_y	α	β	τ_y
Dry	4.03	63.71	28.4	4.42	84.13	18.5
4	3.58	96.76	19.4	6.15	93.80	15.7
7	8.44	113.83	14.1	7.23	117.58	12.2
11	6.08	136.49	12.2	4.14	134.97	11.7

bonding between the oxidized surface functional groups and the epoxy resin. As water condition time increased from 4 to 7 and 11 days, the interfacial shear strength decreased from 32.0 to 50.5 and 57.0% for AS4-DGEBA samples and from 15.2 to 33.9 and 36.6% for AU4-DGEBA samples.

Kaelble et al.¹⁵ predicted the water sensitivity of the fiber/matrix interface based on surface-energy arguments. They showed that water immersion can reduce substantially the critical stress for crack propagation at the interface of graphite/epoxy composites because of their strong polar character. They suggested that the nonpolar interface character was essential for the formation of water-insensitive interfaces. Kaelble et al.¹⁶ showed a 50% reduction of the interlaminar shear strength of

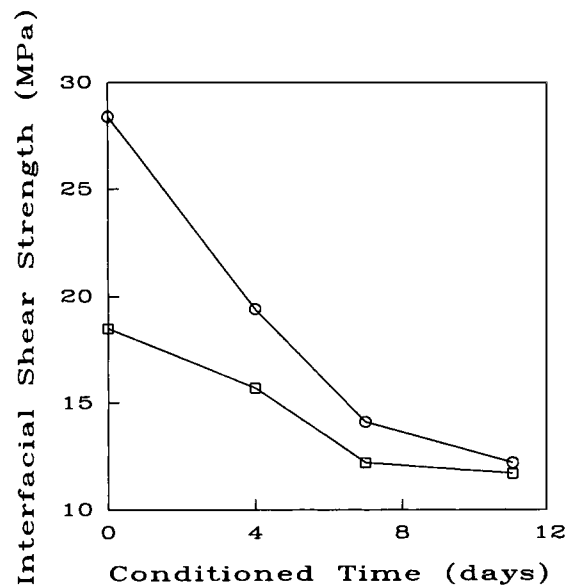


Figure 11 Interfacial shear strength as a function of immersion time in 80°C water (DGEBA + DDA resin and single graphite fiber system). Surface treated fiber (○); nontreated fiber (□).

graphite/epoxy composite after more than 200 h immersion in water at 100°C. They compared the magnitude of the property changes with surface-energy analysis and micromechanics prediction. In addition to the surface energy analysis, the debonding patterns at the interface provided information about the interfacial bond strength change.

In the case of the dry AS4-DGEBA samples, the interfacial bond strengths were so strong that all the fiber breakage was accompanied by epoxy resin cracks during the tensile test. Figure 12(a) and (b) show the typical shapes of epoxy resin cracks after applying tensile stress. The crack shape in Figure 12(a) was most common and sometimes several cracks were gathered around the broken area of a fiber like Figure 12(b). But, as the water-conditioning time increased, the number of fiber breaks accompanying the epoxy resin crack decreased, while the number of fiber breaks without the epoxy resin crack like Figure 12(c) increased. In the case of AU4-DGEBA samples, epoxy resin cracks could not be observed even in dry samples.

The weakening of the interfacial bond strength could also be caused by hygrothermally induced interfacial stresses. Hahn²⁶ suggested that the amount of hygrothermally induced interfacial stress that the fibers could be exposed to from the resin part in an unidirectional composite can be expressed as follows:

$$\sigma_f = - \frac{\phi_m E_f E_m (e_f - e_m)}{(\phi_m E_m + \phi_f E_f)} \quad (8)$$

Here, σ is the stress; E , the Young's modulus; ϕ , the volume fraction; and e , the hygrothermally induced strain. The subscripts f and m are for fiber and resin, respectively. In the case of a Fiberite ANC3K/948A1 composites, $\phi_m = 0.4$, $\phi_f = 0.6$, $E_f = 235$ GPa, $E_m = 3$ GPa, and $e_m = 0.00575$ wt % water at 80°C. From the water sorption test, the equilibrium water uptake was 2.4 wt % at 70°C. If the fiber strain, e_f , is assumed to be negligible and the above data are inserted in eq. (8), the interfacial shear stress acting on the fiber surface from the resin part can be calculated as 27.4 MPa. Thus, the contribution of hygrothermal stress to the weakening of interfacial bonding is not negligible.

It is also shown in Figure 11 that the interfacial shear strength of AS4-DGEBA sample decreased more than that of AU4-DGEBA samples. These results imply that the relatively more polar interface of AS4-DGEBA is more sensitive to water than is the interface of AU4-DGEBA and the chemical

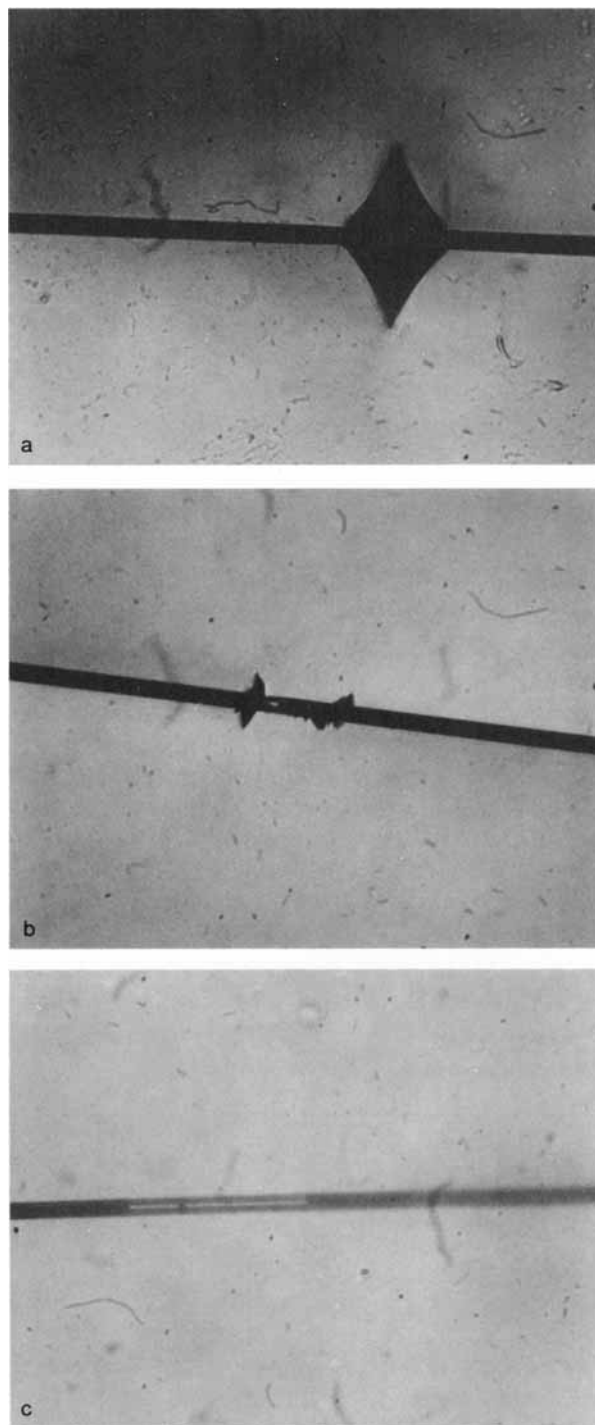


Figure 12 The shapes of fiber breakage after tensile loads.

bonding between oxidized surface of AS4 fiber and DGEBA/DDA epoxy resin did not play an important role on the interfacial shear strength under these conditions.

CONCLUSIONS

This work addressed questions related to the possible debonding between a composite and a fiber due to water penetration in the composite. Studies were carried out with two significantly different composites in an effort to observe conditions of non-Fickian water transport. It is known that non-Fickian water transport describes coupling of diffusional and relaxational processes and is associated with stresses formed throughout the polymer matrix and at the matrix/fiber interface. Thus, highly non-Fickian behavior would lead to debonding.

Sorption kinetics were established at various temperatures for water in Hercules AS4/3501-6 and Fiberite ANC3K/948A1 graphite/epoxy composite samples. The absorption kinetics of water in both composites could be fitted well by a Fickian model at 50, 70, 90, and 100°C. However, non-Fickian (Langmuir)-type two-step sorption was exhibited by water in Fiberite ANC3K/948A1 composite samples at 50 and 70°C.

Internal cracks due to the water absorption were found by scanning electron microscopy and an ultrasonic test in Fiberite ANC3K/948A1 samples conditioned at various temperatures in water (non-Fickian behavior), whereas no cracks were detected in Hercules AS4/948A1 samples conditioned at 100°C water (Fickian behavior).

The single-fiber fragment test revealed that the interfacial shear strength of surface-treated fiber samples is 1.5 times higher than that of nontreated fiber samples. This test also showed that the absorbed water at 80°C reduced significantly the interfacial shear strength of DGEBA/DDA resin-AS4 fiber samples (57%) and DGEBA/DDA resin-AU4 fiber samples (37%).

This work was supported by a grant from the National Science Foundation. M.C.L. was a David Ross Fellow.

REFERENCES

1. T. Takamatsu, *Comp. Polym.*, **1**, 105 (1988).
2. P. Denison, F. R. Jones, and J. F. Watts, in *Interfaces in Polymer, Ceramic, and Metal Matrix Composites*, H. Ishida, Ed., Elsevier, New York, 1988, p. 77.
3. D. Lawing, R. E. Fornes, R. D. Gilbert, and J. D. Memory, *J. Appl. Phys.*, **52**, 5906 (1981).
4. M. K. Antoon, J. L. Koenig, and T. Serafini, *J. Polym. Sci. Polym. Phys. Ed.*, **19**, 1567 (1981).
5. L. W. Jelinski, J. J. Dumais, R. E. Stark, T. S. Ellis, and F. E. Karasz, *Macromolecules*, **16**, 1019 (1983).
6. L. W. Jelinski, J. J. Dumais, R. E. Stark, T. S. Ellis, and F. E. Karasz, *Macromolecules*, **18**, 1091 (1985).
7. M. Woo and M. Piggott, *J. Comp. Tech. Res.*, **9**, 101 (1987).
8. A. Apicella, L. Nicolais, and C. de Cataldis, *Adv. Polym. Sci.*, **66**, 189 (1985).
9. A. Apicella, R. Tessieri, and C. de Cataldis, *J. Membr. Sci.*, **18**, 211 (1984).
10. C. H. Shen and G. S. Springer, *J. Compos. Mater.*, **10**, 2 (1976).
11. S. Neumann and G. Marom, *J. Compos. Mater.*, **21**, 68 (1987).
12. N. R. Farrar and K. H. G. Ashbee, in *Resins for Aerospace*, R. B. Vinson, Ed., ACS Symposium Series 132, American Chemical Society, Washington, DC, 1980.
13. N. R. Farrar and K. H. G. Ashbee, *J. Phys. D Appl. Phys.*, **11**, 1009 (1978).
14. B. Dewimille and A. R. Bunsell, *Composites*, **35** (1983).
15. D. H. Kaelble, P. J. Dynes, and E. H. Cirlin, *J. Adhesion*, **6**, 23 (1974).
16. D. H. Kaelble, P. J. Dynes, and L. W. Crane, *J. Adhesion*, **7**, 25 (1974).
17. T. K. Tsotsis and Y. Weitsman, *J. Compos. Mater.*, **24**, 483 (1990).
18. M. C. Lee and N. A. Peppas, *J. Compos. Mater.*, to appear.
19. D. H. Kaelble, P. J. Dynes, L. W. Crane, and L. Maus, *J. Adhesion*, **5**, 211 (1975).
20. D. H. Kaelble, in *Resins for Aerospace*, R. B. Vinson, Eds., ACS Symposium Series 132, American Chemical Society, Washington, DC, 1980.
21. W. J. Mikols, J. C. Seferis, A. Apicella, and L. Nicolais, *Polym. Compos.*, **3**, 118 (1982).
22. P. S. Chua, *SAMPE Q.*, **18**, 10 (1987).
23. A. Apicella, L. Nicolais, and C. Cargfana, in *The Role of Polymeric Matrix in the Processing and Structural Properties of Composite Materials*, J. C. Seferis and L. Nicolais, Eds., Plenum Press, New York, 1983, p. 215.
24. A. Kelly and W. R. Tyson, *J. Mech. Phys. Solids*, **13**, 329 (1965).
25. L. T. Drzal, M. J. Rich, J. D. Camping, and W. J. Park, in *Proceedings of the Conference of the RP/Composites Institute*, 1980, Paper 20-C, p. 1.
26. H. T. Hahn, *J. Comp. Mater.*, **10**, 266 (1976).

Received February 5, 1992

Accepted April 24, 1992